

Resonant Spin-Flavor Precession Solution to the Solar Neutrino Problem and electron antineutrinos from the Sun

A.A. Bykov ^{b 1}, **V.Yu. Popov** ^{b 2}, **T.I. Rashba** ^{a 3},
and **V.B. Semikoz** ^{a 4}

^a *The Institute of Terrestrial Magnetism, Ionosphere and Radio Wave Propagation of the Russian Academy of Sciences, IZMIRAN, Troitsk, Moscow region, 142190, Russia*

^b *Department of Physics, Moscow State University, 119899, Moscow, Russia*

Abstract

We have found allowed Δm^2 , μB_{\perp} , $\sin^2 2\theta$ – regions for the Resonant Spin-Flavor Precession Solution (RSFP) [1] to the Solar Neutrino Problem (SNP) fitted with data of all acting solar neutrino experiments.

The typical mass difference region $\Delta m^2 \sim 5 \cdot 10^{-9} - 2 \cdot 10^{-8}$ eV² varying in dependence on the mixing $0 \leq \sin^2 2\theta \lesssim 0.05$ is allowed for some discrete magnetic field regions in a wide range $30 \text{ kG} \lesssim B_{\max} \lesssim 300 \text{ kG}$ for the fixed neutrino transition magnetic moment $\mu/10^{-11}\mu_B = \mu_{11} = 1$ (free unknown parameter) and for different regular field profiles. Here B_{\max} is the maximum value of a regular large-scale magnetic field $B(r)$ within the convective zone and the upper value $B_{\max} \simeq 300 \text{ kG}$ is chosen from some known MHD constraints [2].

Except of the first allowed range with the lowest field strength $30 \text{ kG} \lesssim B_{\max} \lesssim 70 \text{ kG}$ (for the same $\mu_{11} = 1$) the values B_{\max} within other discrete allowed regions depend essentially on the profile $B_{\perp}(r)$ of a regular magnetic field in the convective zone of the Sun.

For non-zero neutrino mixing ($s_2^2 = \sin^2 2\theta \neq 0$) one can find at 99.9% CL ($\pm 3\sigma$) an upper limit on the mixing, $s_2^2 \leq s_{2\max}^2 \sim 0.2$, originated by the non-observation of electron antineutrinos in the capture reaction $\bar{\nu}_e p \rightarrow n e^+$ in the Superkamiokande (SK) detector ($\Phi_{\bar{\nu}} \lesssim 0.035\Phi_{\nu_B}$, $E_{\nu} \gtrsim 8.3 \text{ MeV}$ [3]). This limit occurs also sensitive to the magnetic field parameter μB_{\perp} . While at 67% CL ($\pm \sigma$) there is another more stringent upper limit $s_2^2 \leq s_{2\max 1}^2 \sim 0.05$ coming from inconsistency of gallium experiments with others that is also close to the result $s_2 \lesssim 0.25$ [4].

A new allowed region ($\Delta m^2 \approx 10^{-7} \text{ eV}^2$, $\sin^2 2\theta \approx 0.01$) appears in the case of additional assumption that the Homestake data are 1.3 times less than the experimental event rate.

¹E-mail: bikov@math380b.phys.msu.su

²E-mail: popov@math380b.phys.msu.su

³E-mail: rashba@izmiran.rssi.ru

⁴E-mail: semikoz@izmiran.rssi.ru

1 Introduction

The solar neutrino anomaly is strongly established both from five solar neutrino experiments [5] and from the theoretical predictions of the Standard Solar Model (SSM) [6] confirmed by recent helioseismology observations [7]. One of the possible solutions to the SNP is RSFP scenario [1] based on the presence of a non-zero neutrino transition magnetic moment $\mu = \mu_{ij}$, $i \neq j$ [8] is fully consistent with all currently available solar neutrino data.

In the present work we are considering the RSFP solution for various models of regular magnetic fields in the Sun varying three parameters: two fundamental particle physics ones: (i) the neutrino mass difference Δm^2 , (ii) the neutrino mixing $\sin^2 2\theta$ and (iii) the magnetic field parameter $\mu B_\perp(r)$ scaled by the factor μ with the normalized magnetic moment $\mu/10^{-11}\mu_B = \mu_{11}$.

In our plots we put $\mu_{11} = 1$ obeying most known constraints on an active-active neutrino transition magnetic moment including the present laboratory (reactor) bound, $\mu \lesssim 1.8 \times 10^{-10}\mu_B$ [9]. In contrast to the case of a Dirac neutrino, for a Majorana neutrino there is only one more stringent astrophysical constraint coming from the cooling of red giants $\mu \lesssim 3 \times 10^{-12}\mu_B$ [10]. Nevertheless, even this exception does not prevent from our analysis of the RSFP scenario for the Sun since one can easily choose the neighboring allowed B_\perp -regions with higher values of the magnetic field strength (B_{max}) if a more stringent bound on the neutrino magnetic moment is accepted.

2 Magnetic fields in the Sun

It is very little known about magnetic field in the Sun. The MHD models [2] do not exclude the presence of a significant magnetic field (a few hundred kilogauss) at the bottom of the convective zone of the Sun. Moreover, modern dynamo theories forbid large scale magnetic fields in the central part of the Sun with the strength more than 30 Gauss [11]. In the most realistic MHD model of regular magnetic fields in the convective zone one finds the well-known toroidal field in both hemispheres of the Sun [12] which has visible traces in forms of magnetic field loops floating up to active bipolar regions seen on the solar photosphere. The shape and topology of toroidal fields is very complicated and some simplifications of their profile is used for different magnetic field scenarios to solve SNP.

In the present consideration two kinds of magnetic field profiles were used. First one was simple triangle profile of the magnetic field, second - "smooth" profile (see Fig.1). We have varied magnetic field amplitude from a few kilogauss up to 300 kG [2]. Thus, we suppose that magnetic field has a large scale structure and it can be considered as a regular field fixed during total observation time for all neutrino experiments.

3 Master equation

In the case of non-zero vacuum mixing and non-zero transition magnetic moment, the neutrino propagation in the solar medium with a magnetic field can be described by the Schrödinger-like 4×4 evolution equation for two neutrino flavors ν_e and ν_μ with two

helicities

$$i \begin{pmatrix} \dot{\nu}_{eL} \\ \dot{\tilde{\nu}}_{eR} \\ \dot{\nu}_{\mu L} \\ \dot{\tilde{\nu}}_{\mu R} \end{pmatrix} = \begin{pmatrix} V_e - c_2\delta & 0 & s_2\delta & \mu B_+(t) \\ 0 & -V_e - c_2\delta & -\mu B_-(t) & s_2\delta \\ s_2\delta & -\mu B_-(t) & V_\mu + c_2\delta & 0 \\ \mu B_-(t) & s_2\delta & 0 & -V_\mu + c_2\delta \end{pmatrix} \begin{pmatrix} \nu_{eL} \\ \tilde{\nu}_{eR} \\ \nu_{\mu L} \\ \tilde{\nu}_{\mu R} \end{pmatrix}, \quad (1)$$

where $c_2 = \cos 2\theta$, $s_2 = \sin 2\theta$, $\delta = \Delta m^2/4E$ are the neutrino mixing parameters; $\mu = \mu_{ij}$, $i \neq j$, is the neutrino active-active transition magnetic moment; $B_\pm = B_x \pm iB_y$, are the regular magnetic field components which are perpendicular to the neutrino trajectory in the Sun; $V_e(t) = G_F \sqrt{2}(\rho(t)/m_p)(Y_e - Y_n/2)$ and $V_\mu(t) = G_F \sqrt{2}(\rho(t)/m_p)(-Y_n/2)$ are the neutrino vector potentials for ν_{eL} and $\nu_{\mu L}$ in the Sun given by the abundances of the electron ($Y_e = m_p N_e(t)/\rho(t)$) and neutron ($Y_n = m_p N_n(t)/\rho(t)$) components and the SSM density profile $\rho(t) = 250 \text{ g/cm}^3 \exp(-10.54t)$ [13].

Using the experimental data and errors one can find common regions for the neutrino mixing and for magnetic field parameters that obey solutions for all experiments. These regions are named "allowed". All presented plots except of some cases are made at 95% C.L. (2σ).

4 Results and discussion

We have found allowed Δm^2 , μB_\perp , $\sin^2 2\theta$ – regions in the case of the RSFP solution to the SNP [1]. These results are fitted with total rates (Figures 2-7) of all acting solar neutrino experiments such as Homestake, Kamiokande, SAGE, GALLEX, SuperKamiokande [5]:

Experiment	ratio DATA/BP98
Homestake	0.33 ± 0.032
GALLEX+SAGE	0.568 ± 0.076
SuperKamiokande	$0.470 \pm 0.008 \pm 0.013$

Here BP98 are the theoretical predictions of the SSM [6].

All allowed regions have squared mass difference $\Delta m^2 \approx 5 \cdot 10^{-9} \text{ eV}^2 - 2 \cdot 10^{-8} \text{ eV}^2$ (Figures 2-5). In this case neutrinos have resonant spin-flavor conversions in the convective zone. If neutrinos would have much bigger mass difference (up to the MSW solution $\Delta m_{MSW}^2 \approx 10^{-5} \text{ eV}^2$) resonant points are deep in the Sun core (less than 0.3 of the Sun radius), while no significant magnetic fields are expected there [11].

Allowed regions are some discrete areas in a wide range of magnetic field amplitude values B_{max} changing from 30 kG to 300 kG for the fixed neutrino transition magnetic moment μ ($\mu_{11} = 1$) and for the regular magnetic field profiles considered here. Allowed regions are periodical over the magnetic field amplitude B_{max} . This result can be explained in the framework of the simplest model: constant magnetic field in the convective zone [14]. In this case the probability of $\nu_{eL} \rightarrow \nu_{\mu R}$ conversion is

$$P = \frac{(2\mu B_\perp)^2}{(V - \Delta \cos 2\theta)^2 + (2\mu B_\perp)^2} \sin^2 \left(\sqrt{(V - \Delta \cos 2\theta)^2 + (2\mu B_\perp)^2} \frac{\Delta r}{2} \right), \quad (2)$$

where $\Delta = \Delta m^2 / 2E$, $V = V_e + V_\mu$, Δr is the effective width of the magnetic field region in the convective zone. As one can see in Fig.1 the effective width of the triangle profile is a little wider than the effective width of "smooth" profile. Hence both the periodicity of allowed regions (Fig.2 and Fig.3) and their dependence on the magnetic field profile can be explained from Eq.(2) .

Let us emphasize that first allowed regions (minimal values of magnetic fields, $B_{max} \approx 50$ kG) both for triangle (Fig.2) and "smooth" (Fig.3) profiles are very similar, because in the case of small magnetic fields the probabilities depend poorly on a shape of the profile.

Allowed solutions depend very significantly on the neutrino mixing angle (Fig.4 and Fig.5). There are two trends. First one is the disappearance of allowed regions with the increase of mixing angle. The upper limit for mixing angle is $\sin^2 2\theta \approx 0.05$. One concludes that RSFP solution is possible for small mixing angle cases only [4]. Second trend is the disappearance of allowed regions in the case of non-zero mixing for large magnetic field amplitudes although the small magnetic field case is still alive.

The non-observation of electron antineutrinos in the capture reaction $\bar{\nu}_e p \rightarrow ne^+$ in the SuperKamiokande (SK) detector ($\Phi_{\bar{\nu}} \lesssim 0.035\Phi_{\nu_B}$, $E_\nu \gtrsim 8.3$ MeV [3]) gives additional limit on neutrino mixing angles. The antineutrino SK limit [3] bounds the mixing ($s_2^2 = \sin^2 2\theta \leq 0.2$) at 99.9% C.L. ($\pm 3\sigma$) (Fig.6). This limit occurs also sensitive to the magnetic field parameter μB_\perp . The bound is more stringent for larger magnetic fields than for the small ones.

All above mentioned results are in a good agreement with [4, 15, 16].

A new allowed region appears if the additional assumption is taken into account that the Homestake data are 1.3 times less than the experimental event rate [5, (Homestake)]. In this case ($f_{Cl} = 1.3$ [3]) the squared mass difference is $\Delta m^2 \approx 10^{-7}$ eV² and the mixing is $\sin^2 2\theta \approx 0.01$ (Fig.7).

To conclude the RSFP solution to SNP has a good fit for rates observed in all acting neutrino experiments. This fit is not worse than for other solutions such as MSW [17] or vacuum oscillation solution [18]. Since a sizable neutrino transition moment is not forbidden and due to the existence of efficient solar magnetic field, the RSFP solution is still one of the possible solutions to SNP.

Acknowledgments

Authors thank the RFBR grants 97-02-16501, 99-02-26124, T.I.R. and V.B.S. thank the INTAS grant 96-0659.

References

- [1] E. Kh. Akhmedov, Phys. Lett. B 213 (1988) 64; C.-S. Lim and W.J. Marciano, Phys. Rev. D 37 (1988) 1368.
- [2] E.N. Parker, *Cosmological Magnetic Fields*, Oxford University Press, Oxford, 1979; D.W. Hughes in *Advances in Solar System Magnetohydrodynamics*, ed. by E.R.

Priest, Cambridge University Press, 1991; Ya.A. Zeldovich, A.A. Ruzmaikin, D.D. Sokoloff, *Magnetic fields in astrophysics*, Cordon and Breach, N.Y., 1983

- [3] G. Fiorentini, M. Moretti and F.L. Villante, hep-ph/9707097
- [4] E.Kh. Akhmedov, "The neutrino magnetic moment and time variations of the solar neutrino flux", Preprint IC/97/49, Invited talk given at the 4-th International Solar Neutrino Conference, Heidelberg, Germany, April 8-11, 1997. E.Kh. Akhmedov, A. Lanza and S.T. Petcov, Phys. Lett. B303 (1993) 85.
- [5] K. Lande (Homestake Collaboration) in *Neutrino '98*, Proceedings of the XVIII International Conference on Neutrino Physics and Astrophysics, Takayama, Japan, 4-9 June 1998, edited by Y. Suzuki and Y. Totsuka, to be published in Nucl. Phys. B (Proc. Suppl.); Y. Fukuda et al. (Kamiokande Collaboration), Phys. Rev. Lett. 77 (1996) 1683; V. Gavrin (SAGE Collaboration) in *Neutrino '98*; T. Kirsten (GALLEX Collaboration) in *Neutrino '98*; Y. Suzuki (SuperKamiokande Collaboration) in *Neutrino '98*;
- [6] J.N.Bahcall, S.Basu, M.H.Pinsonneault, Phys.Lett.B433 (1998)1.
- [7] V. Berezinsky, astro-ph/9710126, invited lecture at 25th International Cosmic Ray Conference, Durban, 28 July - 8 August, 1997; V. Castellani, S. Degl'Innocenti, G. Fiorentini, Astron. Astrophys. 271 (1993) 601; W.A. Dziembowski, Bull. Astron. Soc. India 24 (1996) 133; S. Degl'Innocenti, W.A. Dziembowski, G. Fiorentini, B. Ricci, Astropart. Phys. 7 (1997) 77.
- [8] J. Schechter, J.W.F. Valle, Phys. Rev. D24 (1981) 1883; ibid. D25 (1982) 283 (E)
- [9] A.V. Derbin, Yad. Fiz. 57 (1994) 236 (Eng. Transl. in Phys. At. Nucl. 59 (1994) 1171)
- [10] G.G. Raffelt, Phys.Rev.Lett. 64(1990)2856; Phys.Rep. 198(1990)1.
- [11] N. Boruta, Astrophys. J., 458 (1996) 832.
- [12] H. Yoishimura, Astrophys. J., 178 (1972) 863; Astrophys. J. Suppl. Ser., 52 (1983) 363.
- [13] John N. Bahcall, *Neutrino Astrophysics*, Cambridge University Press, 1988, section 6.3.
- [14] A.A. Bykov, V.Yu. Popov, A.I. Rez, V.B. Semikoz, D.D. Sokoloff, hep-ph/9808342.
- [15] M. Guzzo, H. Nunokawa, hep-ph/9810408.
- [16] J. Pulido, E.Kh. Akhmedov, hep-ph/9907339.
- [17] S.P. Mikheev, A.Yu. Smirnov, Sov. J. Nucl. Phys. 42 (1985) 913; Nuovo Cimento C9 (1986) 17; L. Wolfenstein, Phys. Rev. D17 (1978) 2369.
- [18] V.N. Gribov, B.M. Pontecorvo, Phys. Lett. B28 (1969) 493.

Figure captions

Figure 1. Magnetic field profiles.

Figure 2. Ratio DATA/BP98 for all acting experiments (Homestake, SAGE, GALLEX, SuperKamiokande, see Table above) on the plane $\lg \Delta m^2$ (eV 2) and $B_{max}/100$ kG for triangle magnetic field profile and zero mixing angle ($\sin^2 2\theta = 0$) at 95% C.L.

Figure 3. Same as Fig.2 for "smooth" profile and $\sin^2 2\theta = 0$.

Figure 4. Same as Fig.2 for triangle profile and $\sin^2 2\theta = 0.05$.

Figure 5. Same as Fig.2 for "smooth" profile and $\sin^2 2\theta = 0.05$.

Figure 6. Same as Fig.2 for "smooth" profile and $\sin^2 2\theta = 0.2$. Cross-lined zone is the region excluded by the SK antineutrino bound [3].

Figure 7. Same as Fig.2 for triangle profile and $\sin^2 2\theta = 0.01$ and for the case of the increased Homestake flux $f_{Cl} = 1.3$.

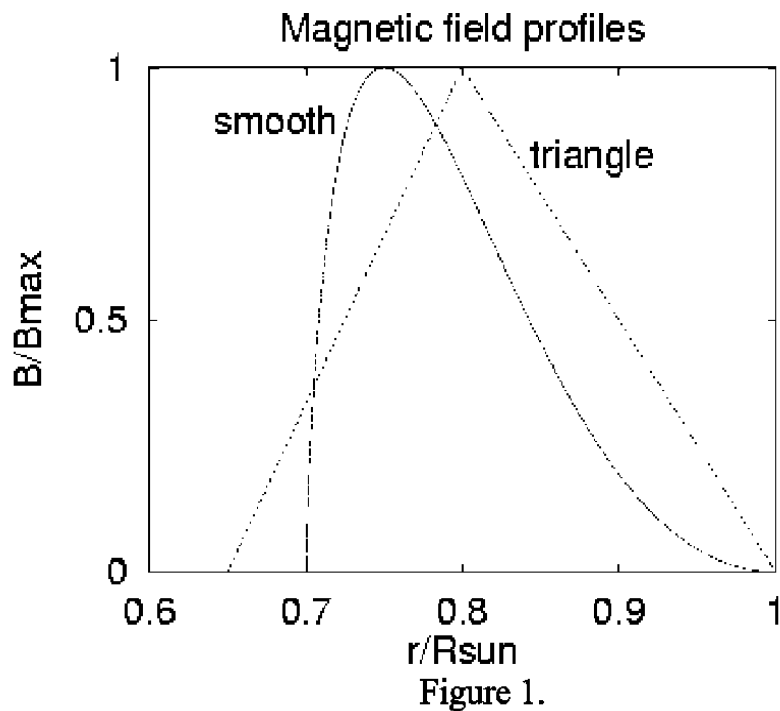


Figure 1.

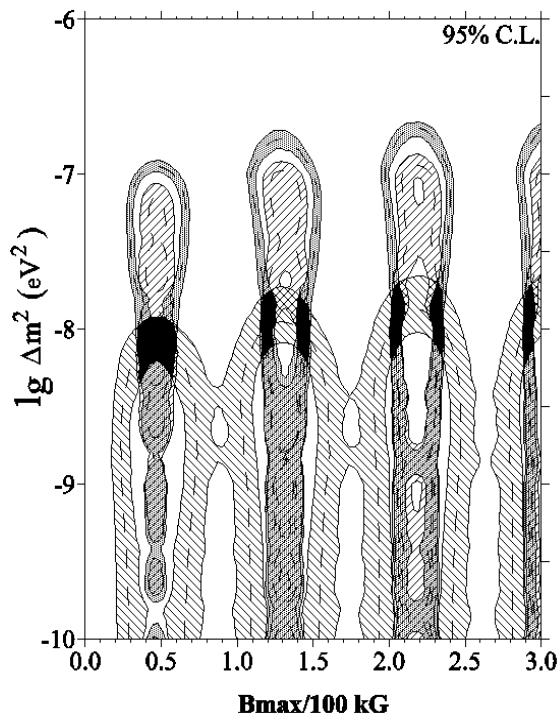


Figure 2.

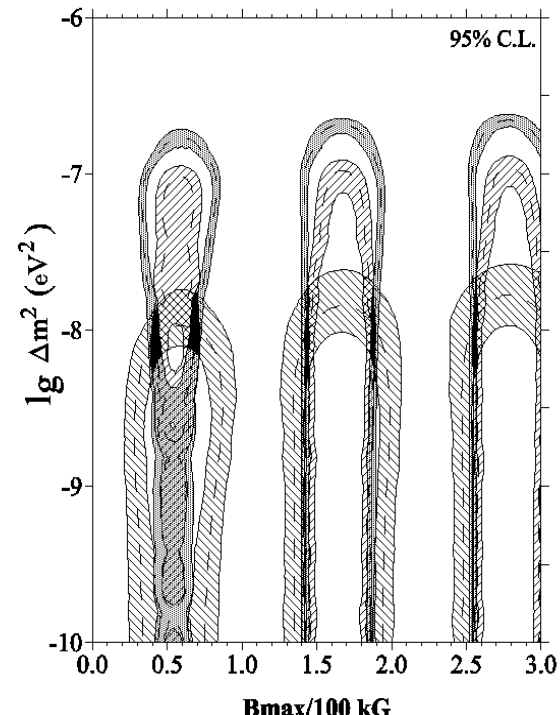


Figure 3.

Homestake	SuperKamiokande	Allowed regions
GALLEX + SAGE	SK bound on antineutrino	

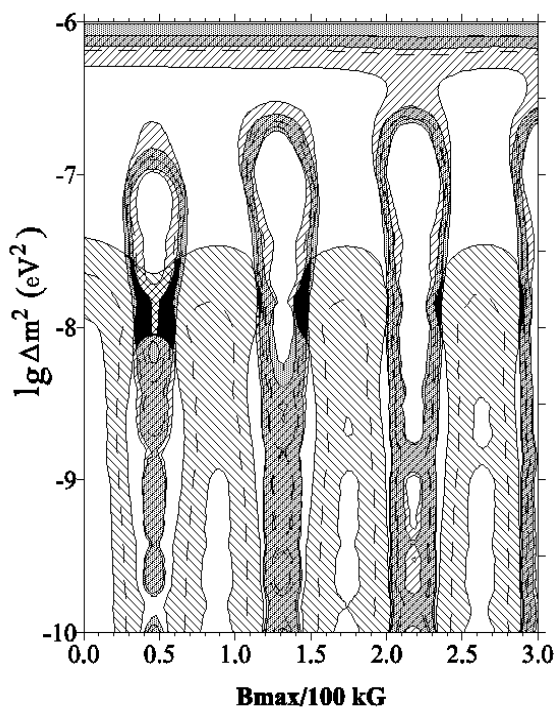


Figure 4.

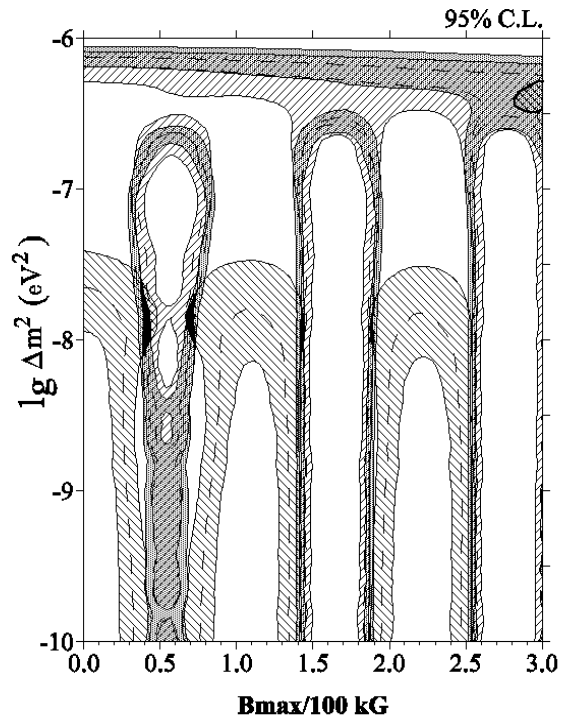


Figure 5.

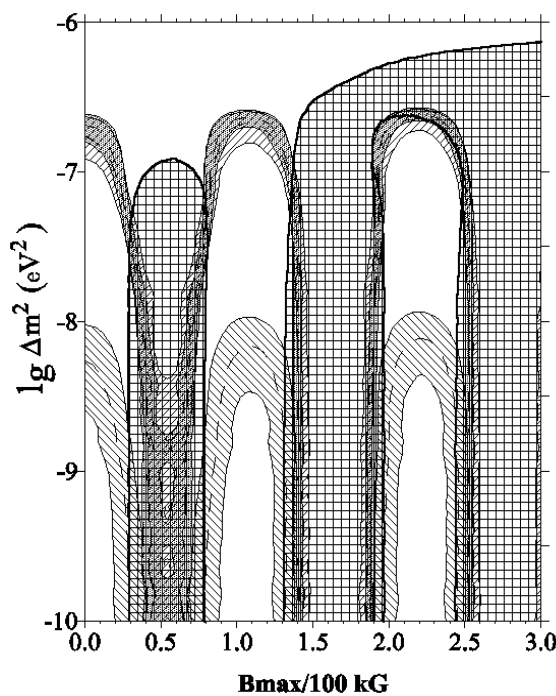


Figure 6.

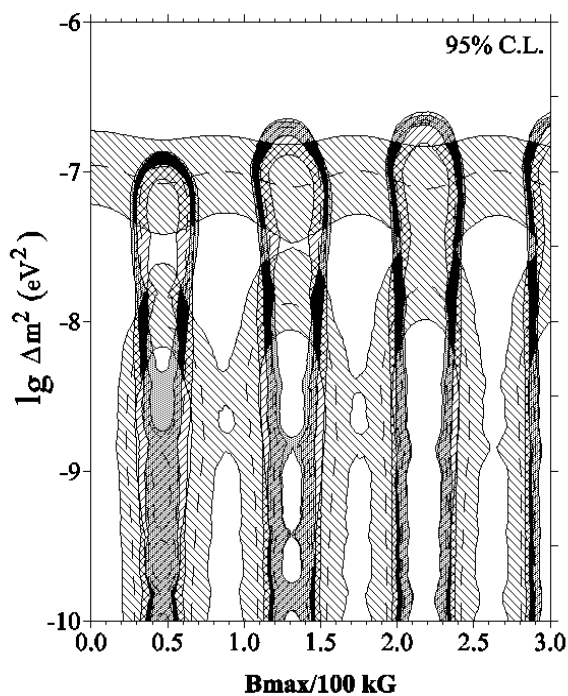


Figure 7.

Homestake	SuperKamiokande	Allowed regions
GALLEX + SAGE	SK bound on antineutrino	